JOURNAL OF MATERIALS SCIENCE 31 (1996) 4859–4863

Crystallization and properties of a perovskite glass-ceramic

JIIN-JYH SHYU, YEONG-SONG YANG
Department of Materials Engineering, Tatung Institute of Technology, Taipei, Taiwan 104

Crystallization and properties of a $PbO–BaO–TiO_2–Al_2O_3–SiO_2–B_2O_3$ glass-ceramic were studied. The primary crystalline phase was bulk-crystallized perovskite titanate. The secondary crystalline phases were a bulk-crystallized transient $PbTi_3O_7$ phase and a surface-crystallized $PbO \cdot Al_2O_3 \cdot 2SiO_2$ phase. As the heating temperature/time increased, the structure of the precipitated perovskite crystals was transformed from cubic to tetragonal, and the measured *c/a* ratio increased to approach a constant value which is lower than that for the strain-free crystal. Moreover, the crystallized amount of perovskite phase first increased to a maximum, then decreased. The results have been explained by a coarsening process of the perovskite particles. With increasing frequency (200–10^5 Hz), the dielectric constant of the crystallized samples ranged from about 80–70. The dielectric constant was mainly determined by the perovskite content.

1. Introduction

Controlled crystallization in glasses has led to the development of glass-ceramic materials with pore-free, fine-grained microstructure and specific properties. Much of the work in the field of glass-ceramics has been done on the thermal and mechanical properties. On the other hand, few investigations have been reported on the high-permittivity glass-ceramics containing a ferroelectric phase, such as $BaTiO_3$ [1–6], $PbTiO_3$ [7–18], and $NaNbO_3$ [19–23]. The features of interest in the ferroelectric glass-ceramics containing $PbTiO_3$ are crystallographic cubic – tetragonal inversion [8–10], crystal composition [8, 10], dielectric constant [9, 14], crystal morphology, and crystallization kinetics [7, 12, 16, 17], etc. It is well known that the properties of a glass-ceramic material are mainly determined by the intrinsic properties of the major crystalline phase. However, often the observed properties of the major crystalline phase show some extent of deviation from its intrinsic properties, mainly due to (i) the effects of the surrounding matrix, (ii) the formation of secondary crystalline phase(s), and (iii) the metastable state of the major crystalline phase. Therefore, a better understanding of the formation and properties of these ferroelectric glass-ceramic materials is needed. In the present paper, the crystallization and dielectric constant of the glass with a composition (mol %) of 39 PbO, 1 BaO, 25 TiO_2, 1 B_2O_3, 9.7 Al_2O_3, 24.3 SiO_2 were investigated.

2. Experimental procedure

2.1. Sample preparation

Well-mixed, dried powder containing appropriate amounts of reagent-grade PbO, $BaCO_3$, TiO_2, B_2O_3, Al_2O_3, and SiO_2 was melted in a platinum crucible for 30 min at 1200 °C and then quenched by pouring it on to a copper plate. The glass was then annealed at 450 °C for 30 min and then furnace-cooled to room temperature. The as-annealed glass was cut by a diamond saw to yield rectangular bars. The samples were heated at 590–800 °C for 0–48 h with a heating rate of 10 K min^{-1}.

2.2. Characterization

The crystallization temperatures were measured using a differential thermal analyser (DTA), on a powder sample in platinum sample holders. The heating rate was 10 K min^{-1}.

Phase identification was conducted by X-ray diffraction (XRD) analysis using powder samples. Measurements were performed on a diffractometer (Model D5000, Siemens, Germany) operating at 40 kV and 15 mA. Continuous scanning was used with a scan speed of 2° min^{-1} and a sampling interval of 0.01° (2θ). Lattice parameter measurements were conducted by using the (1 1 1), (2 0 0), (2 0 2), (3 1 1), (2 2 2), and (4 1 1) lines of the perovskite phase. Step scanning was used with a fix time of 5–15 s for each interval of 0.02° (2θ). The crystallized amount of the perovskite phase was measured by using a silicon internal standard. The integrated intensities of the (1 1 1) lines for both perovskite and silicon were calculated.

The crystallized samples were polished, etched with a solution of 0.5 wt % HNO_3 + 0.4 wt % HF at 25 °C for 60 s, and then coated with a thin film of gold for scanning electron microscopy (SEM) observations (Model ABT-55, Akashi Beam Tech. Corp., Tokyo, Japan).

Crystallized samples were ground and electroded for the dielectric measurement. The frequency

0022–2461 © *1996 Chapman & Hall*

dependence of relative dielectric constant was measured by an LCR meter at 1 V amplitude in the frequency range 200–10^5 Hz. The measurement was conducted at room temperature.

3. Results and discussion

3.1. Thermal analysis

Fig. 1 shows the DTA curve for the annealed glass. The endothermal minimum at about 560 °C was correlated with the glass transition and softening process. The first exothermal peak at about 645 °C probably represented a phase separation process, according to the work done by Kokubo *et al.* [15]. The second exothermal peak at about 657 °C was caused by the crystallization of the major crystalline phase – lead titanate. The broad exotherm at about 769 °C was mainly due to the crystallization of $PbO{\cdot}Al_2O_3{\cdot}2SiO_2$ (PAS_2). The above crystallinity results have been confirmed by XRD analysis.

3.2. Phase identification

Fig. 2 shows typical XRD patterns for the crystallized samples. For the sample heated at 590 °C for 2 h, titanate perovskite phase with cubic structure began to crystallize. The amount of this phase increased as the sample was heated at 680 °C. A minor crystalline phase, $PbO{\cdot}3TiO_2$, also formed. The sample heated at 760 °C for 2 h revealed tetragonal perovskite phase (identified by the $\{hh0\}$ and $\{h00\}$ doublets). Furthermore, lines corresponding to PAS_2 phase developed at 830 °C. Note that the PT_3 peaks decreased as PAS_2 formed, and disappeared as the heating time at 830 °C was increased. This indicates that $PbO{\cdot}3TiO_2$ was a transient phase.

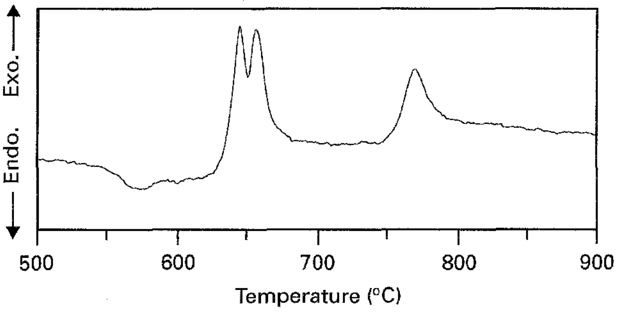

Figure 1 DTA curve for the annealed glass.

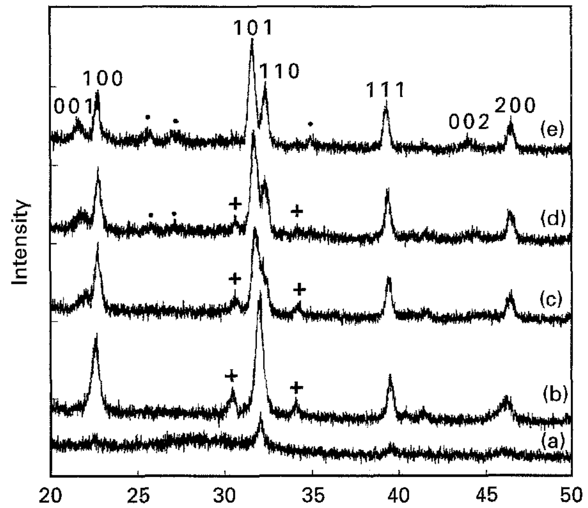

Figure 2 XRD patterns of the samples heated at (a) 590 °C/2 h, (b) 680 °C/2 h, (c) 760 °C/2 h, (d) 830 °C/12 h, and (e) 830 °C/12 h. (hkl) perovskite; (+) PT_3; (●) PAS_2.

3.3. Microstructure

Fig. 3a shows that a surface layer had grown perpendicular to the surface of the sample heated at 830 °C for 2 h. The enlarged micrograph (Fig. 3b) indicates that the surface layer contains branching leaf-like arms which were identified as PAS_2 phase according to the XRD analysis. It was found that the layer growth-rate is constant at a fixed temperature (e.g. 830 °C). Similar microstructures can be seen for most of the crystallized samples. The above result indicates that the crystallization of PAS_2 was surface active.

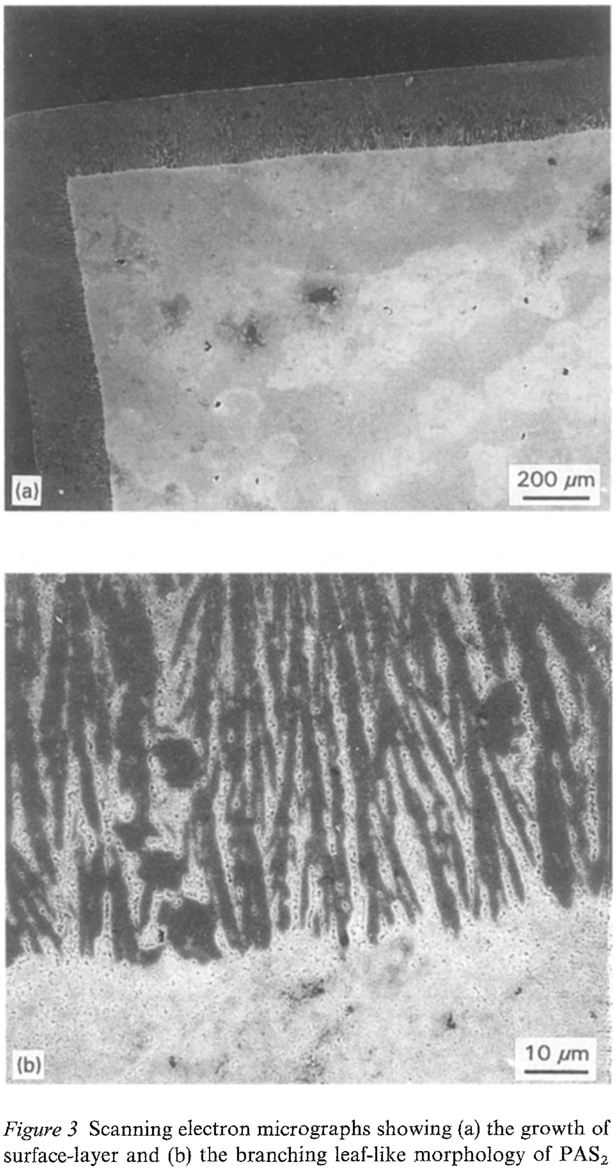

Figure 3 Scanning electron micrographs showing (a) the growth of surface-layer and (b) the branching leaf-like morphology of PAS_2 phase. Sample heated at 830 °C for 2 h.

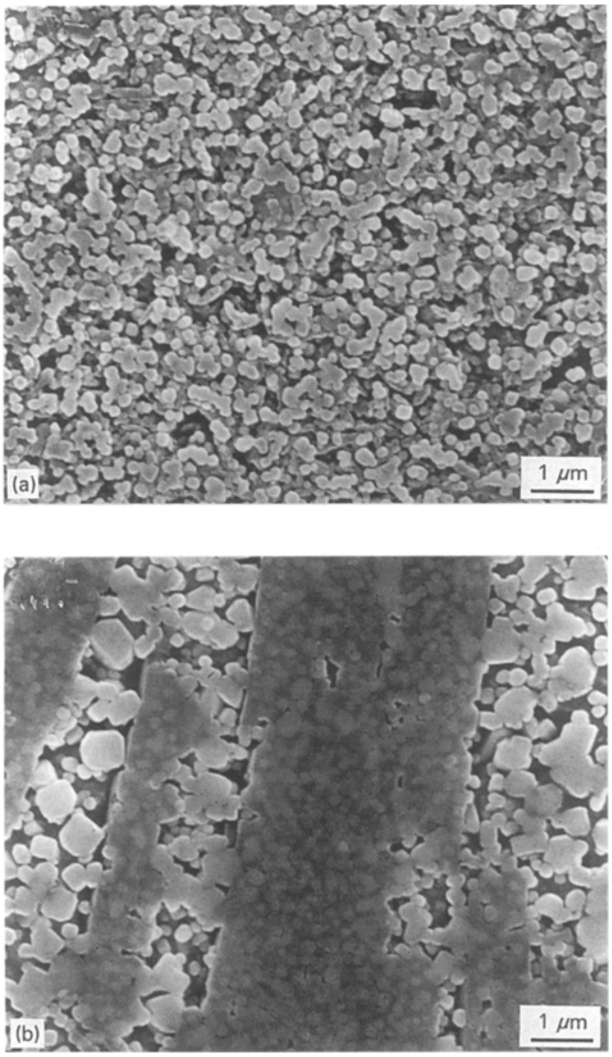

Figure 4 Scanning electron micrographs showing the detailed microstructures of (a) surface-layer region and (b) bulk region. Sample heated at 830 °C for 2 h.

Fig. 4a shows the detailed microstructure in the bulk region of the sample heated at 830 °C for 2 h. Small perovskite particles (about 0.2 μm) uniformly distributed in the matrix. The matrix should be essentially amorphous, distinguished by its severely etched nature. It was found that, as the heating temperature/time increased, the size of the perovskite particles in this region remained nearly unchanged. Fig. 4b shows the detailed microstructure in the surface layer of the same sample. The white particles are perovskite and the grey leaf-like phase is PAS_2. Two kinds of perovskite particles with different sizes can be clearly distinguished: the small ones, which exhibited the sizes close to that observed in the bulk region (Fig. 4a), were trapped in the PAS_2 leaves, and the coarse ones were located between the PAS_2 leaves. As the heating temperature/time increased, the small perovskite particles grew only slightly while the coarse ones grew to a very large size. According to the above results from Fig. 4a and b, it is evident that, as the heating temperature/time increased, growth of the PAS_2 surface layer towards the centre of the sample resulted in two different sizes of perovskite particles. The relative amount of coarse to small perovskite particles increased due to the increased thickness of the surface layer. The above microstructure development is similar in nature to that observed in our previously studied glass-ceramic which has a composition close to the present one [24]. The mechanism for this microstructure development has been discussed in our previous work [24], and would thus be suitable for the present glass. This mechanism suggests that the coarse perovskite particles were formed through an Ostwald ripening process, rather than a primary crystal-growth process. Namely, the smaller perovskite particles dissolve and the larger ones grow.

3.4. *c*/*a* ratio

Fig. 5a and b show the values of *c*, *a*, and *c*/*a* ratio of the tetragonal perovskite phase as a function of heating temperature (for heating time of 24 h) and time (for a heating temperature of 830 °C), respectively. The corresponding values obtained by conducting the same XRD experiment on a commercial, pure $PbTiO_3$ powder are $c = 0.4169$ nm, $a = 0.3895$ nm, and $c/a = 1.065$. It can be seen from both figures that, as the heating temperature/time increased, *a* decreased

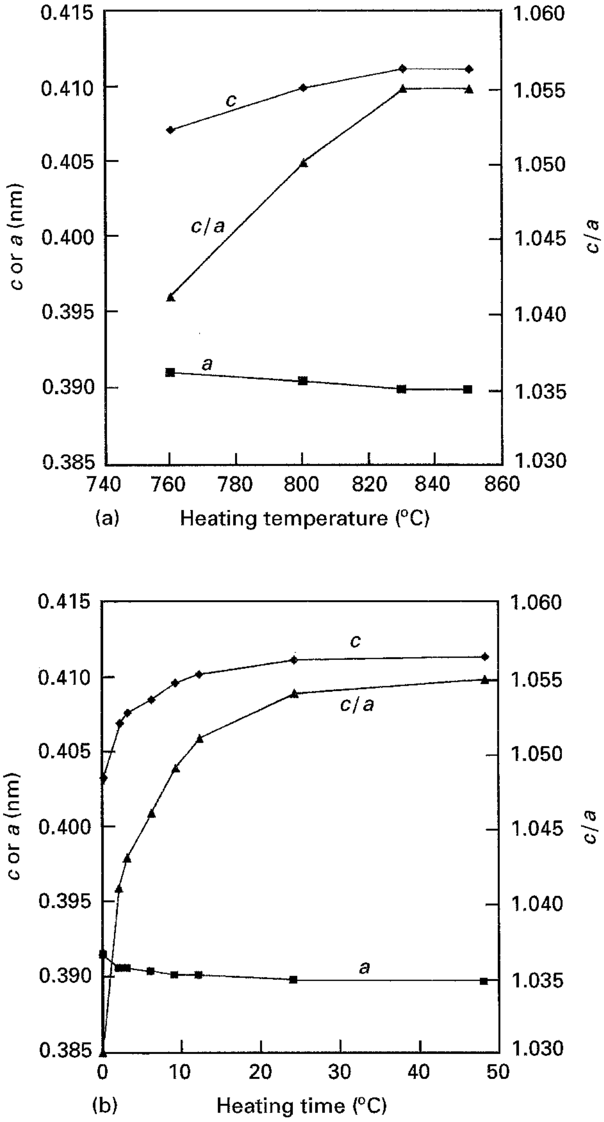

Figure 5 Dependence of lattice constant as a function of (a) heating temperature (for heating time of 24 h) and (b) heating time at 830 °C.

and c and c/a values increased, then these three values approached constants of about 0.3900 nm, 0.4115 nm, and 1.055, respectively. Moreover, the above values are still lower than the corresponding values of the reference $PbTiO_3$ powder, indicating a decreased spontaneous deformation of the perovskite crystals. The above results can be explained by the aforementioned microstructure development. As the crystallized samples were cooled through the Curie temperature, the spontaneous deformation of the ferroelectric phase can be restricted by the external stress applied by the surrounding rigid matrix. A small crystal size implies a high external stress and thus reduces the spontaneous deformation (c/a ratio) [8–10, 25–27]. As a result, in the early stages of crystallization, the perovskite phase was small grained and thus exhibited low c/a ratio. As the heating temperature/time increased, the growth of the surface layer significantly increased the relative amount of coarse to fine perovskite particles (and thus the average size). As a result, an increase in c/a ratio can be seen. Moreover, the final c/a ratio obtained (1.055) was still lower than the reference value of 1.065, indicating that the particle-size effect was still active. Another possible explanation for the above result could be attributed to chemical effect. Substantial impurities might be present in the initial, low-temperature perovskite phase, reducing the c/a ratio and possibly even suppressing the cubic-to-tetragonal phase transition. Epitaxial growth of $PbTiO_3$ could then occur on the nucleating phase, resulting in an increase in the c/a ratio as a function of increasing temperature/time. Further work is needed to confirm this point.

3.5. Crystallinity amount of the perovskite phase

The weight percentage of the perovskite phase crystallized as a function of heating time at 830 °C is shown in Fig. 6. It can be seen that the perovskite content increased initially to a maximum of about 30 wt % at 6 h, then decreased continuously to about 25 wt % at 12 h. Note that this heating temperature (830 °C) is much lower than the melting temperature of the perovskite crystal, therefore the crystal melting process should not be the cause. According to the aforementioned mechanism for microstructure development, the coarse perovskite particles were formed through an Ostwald ripening process, i.e. in the regions between PAS_2 leaves the smaller perovskite particles dissolved and then precipitated on to the large ones. According to the SEM observation (not shown), the dissolution and coarsening of the perovskite particles proceeded even as the bulk region had been fully replaced by the surface layer. It is thus suggested that this process should be responsible for the decrease in amount of perovskite phase, as seen in Fig. 6.

3.6. Dielectric constant

Fig. 7 shows the relative dielectric constant as a function of frequency for the samples heated at 830 °C for various times. With increasing frequency, the dielectric constant decreased smoothly from 73–86 to 65–74. The range of dielectric constant for the present glass-ceramics is slightly higher than that reported by Wu and Zhu [28], and is lower than that for $PbTiO_3$ ceramic (about 133 [29]). It was found that the

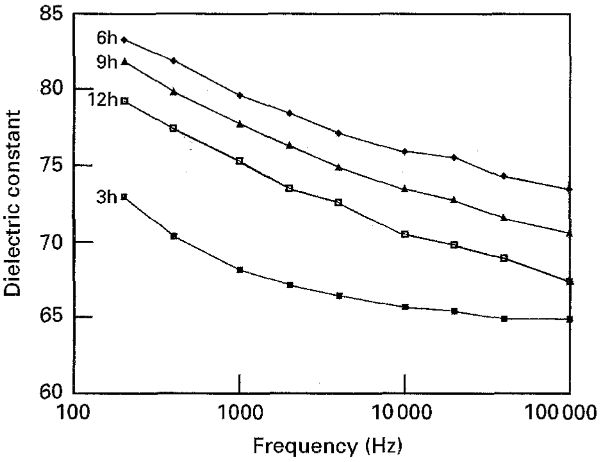

Figure 7 Dependence of dielectric constant as a function of frequency for the samples heated at 830 °C for various times.

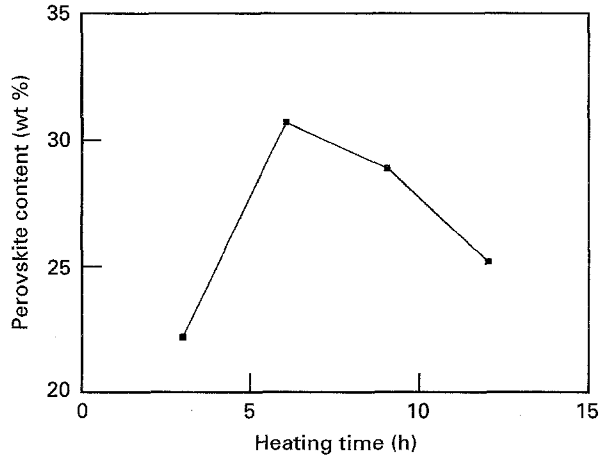

Figure 6 Weight percentage of perovskite phase formed as a function of heating time at 830 °C.

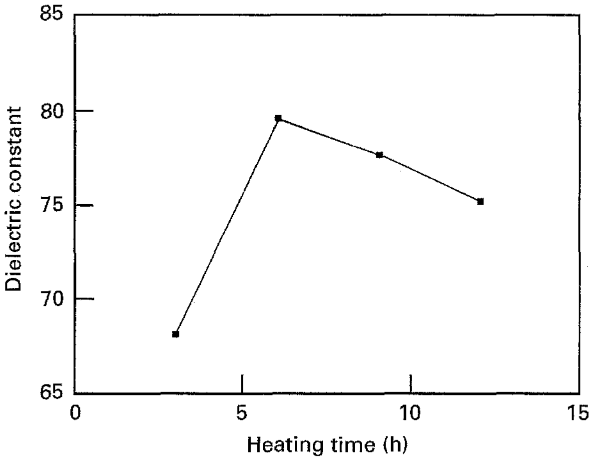

Figure 8 Dependence of dielectric constant at 1 kHz as a function of heating time for the samples heated at 830 °C.

dissipation factor (not shown) decreased with the increasing frequency, especially in the lower frequency range. This suggests that there were some space-charge effects, probably arising from residual glassy phases. The dependence of dielectric constant at 1 kHz as a function of the heating time at 830 °C is shown in Fig. 8. It is well known that the observed properties of a glass-ceramic material are determined by the relative amounts and properties of the phases present. It can be seen that the trend of dielectric constant is consistent with that of perovskite content (Fig. 6), indicating that the dielectric constant of the present glass-ceramics is mainly controlled by the perovskite content.

4. Conclusions

1. The primary crystalline phase was bulk-crystallized perovskite titanate. The secondary crystalline phases were a bulk-crystallized transient $PbTi_3O_7$ phase and a surface-crystallized $PbO{\cdot}Al_2O_3{\cdot}2SiO_2$ phase.

2. As the heating temperature/time increased, the structure of the precipitated perovskite crystals was transferred from cubic to tetragonal, and the measured c/a ratio increased to approach a constant value which is lower than that for the strain-free crystal. Moreover, the crystallized amount of the perovskite phase first increased to a maximum then decreased. The above results are explained by a coarsening process of the perovskite particles.

3. With the increasing frequency (200–10^5 Hz), the dielectric constant of the crystallized samples ranged from about 80–70. The dielectric constant was mainly determined by the perovskite amount.

Acknowledgement

The authors thank the National Science Council of the Republic of China for financial support under Contract NSC 82-0115-E036-074.

References

1. A. HERCZOG, *J. Am. Ceram. Soc.* **67** (1984) 484.
2. *Idem, ibid.* **47** (1964) 107.
3. T. KOKUBO, S. SAKKA and M. TASHIRO, *Yogyo Kyokaishi* **74** (4) (1966) 128.
4. T. KOKUBO, C. KUNG and M. TASHIRO, *ibid.* **76**(4) (1968) 89.
5. D. HULSENBERG and J. LEHMANN, *Silikattechnik* **34**(3) (1983) 74.
6. A. BHARGAVA, J. E. SHELBY and R. L. SNYDER, *J. Non-Cryst. Solids* **102** (1988) 136.
7. M. A. C. G. Van de GRAAF, J. C. LODDER and A. J. BURGGRAAF, *Glass Technol.* **15**(6) (1974) 143.
8. D. G. GROSSMAN and J. O. ISARD, *J. Mater. Sci.* **4** (1969) 1059.
9. T. KOKUBO and M. TASHIRO, *J. Non-Cryst. Solids* **13** (1973/74) 328.
10. S. M. LYNCH and J. E. SHELBY, *J. Am. Ceram. Soc.* **67** (1984) 424.
11. F. W. MARTIN, *Phys. Chem. Glasses* **6**(4) (1965) 43.
12. C. K. RUSSELL and C. G. BERGERON, *J. Am. Ceram. Soc.* **48** (1965) 162.
13. D. G. GROSSMAN and J. O. ISARD, *ibid.* **52** (1969) 230.
14. *Idem, J. Phys. D.* **3** (1970) 1058.
15. T. KOKUBO, H. NAGAO and M. TASHIRO, *Yogyo Kyokaishi* **77** (1969) 293.
16. C. G. BERGERON and C. K. RUSSELL, *J. Am. Ceram. Soc.* **48** (1965) 115.
17. W. K. TREDWAY, S. H. RISBUD and C. G. BERGERON, in "Nucleation and Crystallization in Glasses, Advances in Ceramics", Vol. 4, edited by J. H. Simmons, D. R. Uhlmann and G. H. Beall (American Ceramic Society, Westerville, OH, 1982) p. 163.
18. M. TAKASHIGE, T. MITSUI, T. NAKAMURA, Y. AIKAWA and M. S. JANG, *Jpn J. Appl. Phys.* **20** (1981) L159.
19. N. F. BORELLI, A. HERCZOG and R. D. MAURER, *Appl. Phys. Lett.* **7** (1965) 117.
20. N. F. BORELLI, *J. Appl. Phys.* **38** (1967) 4243.
21. N. F. BORELLI and M. M. LAYTON, *J. Non-Cryst. Solids* **6** (1971) 197.
22. M. M. LAYTON and A. HERCZOG, *J. Am. Ceram. Soc.* **50** (1967) 369.
23. *Idem, Glass Technol.* **10**(2) (1969) 50.
24. J. J. SHYU and Y. S. YANG, *J. Am Ceram. Soc.* **78** (1995) 1463.
25. K. UCHINO, E. SADANAGA, K. OONISHI, T. MOROHASHI and H. YAMAMURA, in Ceramic Dielectrics: Composition, Processing and Properties, Ceramic Transactions 8", edited by H. C. Ling and M. F. Yan (American Ceramic Society, Westerville, OH, 1990) p. 107.
26. G. ARIT, D. HENNINGS and G. DE WITH, *J. Appl. Phys.* **58** (1985) 1619.
27. A. YAMAJI, Y. ENOMOTO, K. KINOSHITA and T. MURAKAMI, *J. Am. Ceram. Soc.* **60**(3–4) (1977) 97.
28. M. WU and P. ZHU, *J. Non-Cryst. Solids* **84** (1986) 344.
29. I. UEDA, *Jpn J. Appl. Phys.* **11** (1972) 450.

Received 17 March 1995
and accepted 13 February 1996